

$$h \frac{d(\Delta\omega^*)}{dt} = -\frac{k}{x_{st}^*} \text{Im} \left[(\underline{\Psi}_s^*) \cdot \Delta\underline{\Psi}_r^{/*} + \underline{\Psi}_r^{/*} \cdot \Delta(\underline{\Psi}_s^*)^* \right]$$

where s is the operational variable.

It must also be noticed that for simplifying the writing and for not producing confusions, both in the previous relation and in the following ones, it has been given up both to indicate the quantities depending on s and to note them with capitals.

If it is considered that $\Delta\omega^*$ is not less than 0,1 in the previous relations, the following approximations may be made:

$$j\underline{\Psi}_s^* = 1 \text{ and } j\underline{\Psi}_r^{/*} = k \tag{4}$$

This way, the first two relations from Eqs. (3) become:

$$0 = (s_{ks} + j\omega_s^* + s)\Delta\underline{\Psi}_s^* - s_{ks} \cdot k \cdot \Delta\underline{\Psi}_r^{/*} \tag{5}$$

$$k(\Delta\omega^* - \Delta\omega_s^*) = -s_{kr} \cdot k \cdot \Delta\underline{\Psi}_s^* + (s_{kr} + s)\Delta\underline{\Psi}_r^{/*}$$

The analysis of these relations can be simplified if it is considered that $R_s \cong 0$. But this simplifying hypothesis leads to satisfactory results only inside the interval $\omega_s^* \in (0,5 \div 1)$.

So it is imposed to analyze the situation when $R_s \neq 0$, but considering that the studied phenomenon is linearized.

In this purpose it is considered that the motor operated without load before modifying the frequency. In this situation, owing to the low frequency of the rotor current, its active component may be neglected.

Thus, one can write:

$$\Delta i_r^{/*} = \Delta i_{dr}^{/*} + j\Delta i_{qr}^{/*} \cong \Delta i_{dr}^{/*} = \frac{\Delta \Psi_r^{/*} - k\Delta \Psi_s^*}{dx_s^*} \tag{6}$$

The following relation is obtained by computations, by solving the system equation (5) relatively to $\Delta \Psi_s^*$ and $\Delta \Psi_r^{/*}$, by replacing these relations in equation (6):

$$\Delta i_{dr}^{/*} = \frac{s + j\omega_s^* + \varepsilon}{s^2 + (s_{ks} + s_{kr} + j\omega_s^*)s + s_{kr}(\varepsilon + j\omega_s^*)} \cdot k(\Delta\omega^* - \Delta\omega_s^*) \tag{7}$$

where the following notation has been used:

$$\varepsilon = (1 - k^2)s_{ks} = \frac{r_s^*}{x_s^*} = \frac{r_s^*}{x_r^{/*}} \tag{8}$$

When $\omega_s^* \geq 0,1$ it results that it can be considered (with approximation):

$$(\underline{\Psi}_s^*)^* = 1 \text{ and } \underline{\Psi}_r^{/*} = -jk \tag{9}$$

In these conditions, the following relation is obtained by applying Laplace transformation to the equation (9):

$$hs \cdot \Delta\omega^* = -\frac{k}{x_{st}^*} \text{Re}(\Delta\underline{\Psi}_r^{/*} - k\Delta\underline{\Psi}_s^*) \tag{10}$$

or, equivalently

$$hs \cdot \Delta\omega^* = -\frac{k}{x_{st}^*} \text{Re}(\Delta\underline{\Psi}_{dr}^{/*} - k\Delta\underline{\Psi}_{ds}^*) \tag{11}$$

respectively

$$hs \cdot \Delta\omega^* = -k\Delta i_{dr}^{/*} \tag{12}$$

III. SIMULATIONS. QUANTITATIVE RESULTS

Further on, for the study of the induction motor stability, the equations (7) and (12) established before are used. The first relation can be written in the form [6]:

$$\Delta\omega^* = -\frac{k}{hs} \cdot \Delta i_{dr}^{/*} \Leftrightarrow \Delta\omega^* = G_1(s) \cdot \Delta i_{dr}^{/*} \tag{13}$$

$$G_1(s) = -\frac{k}{hs} \tag{14}$$

The second relation is processed analogously:

$$\Delta i_{dr}^{/*} = G_2(s) \cdot (\Delta\omega_s^* - \Delta\omega^*) \tag{15}$$

where

$$G_2(s) = \frac{s + j\omega_s^* + \varepsilon}{s^2 + (s_{ks} + s_{kr} + j\omega_s^*)s + s_{kr}(\varepsilon + j\omega_s^*)s + s_{kr}(\varepsilon + j\omega_s^*)} \cdot k \tag{16}$$

The following configuration can be drawn by using equations (13) and (15).

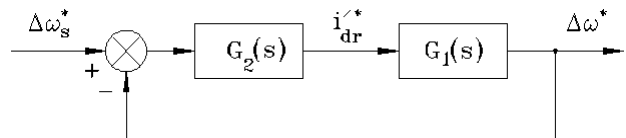


Fig. 1 Machine block scheme in the mentioned situation

Further on it is possible to pass to the stability study in our concrete case by using all these introductive notions. This analysis will be made with the help of a Matlab program conceived on the basis of the scheme depicted in fig. 1 and of

the equations (13), (14), (15) and (16).

The following graphics have been obtained by running this program.

$$x_{1m}^* = 2,0623; \quad x_{st}^* = 0,2456; \quad x_{rt}^* = 0,2451; \quad s_{ks} = 0,4026;$$

$$s_{kr} = 0,2958; \quad k = 0,9414; \quad h = 32,4; \quad \varepsilon = 0,0458.$$

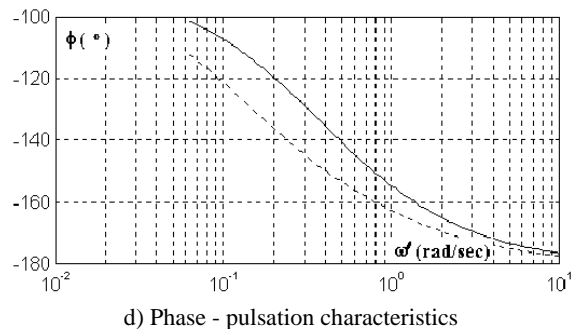
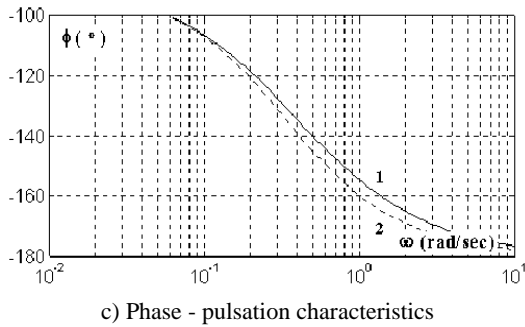
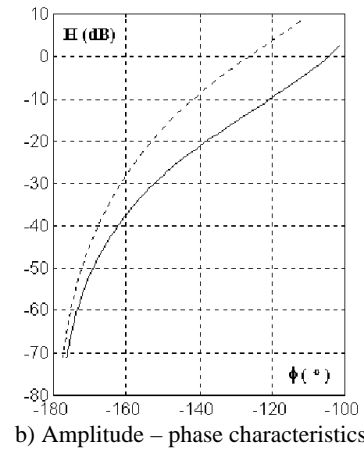
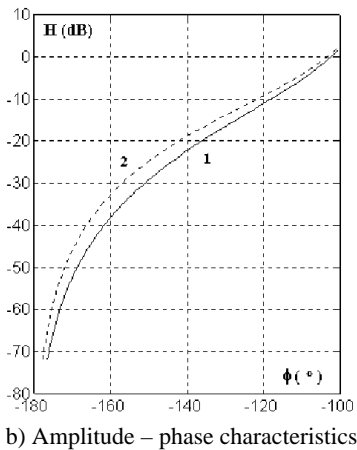
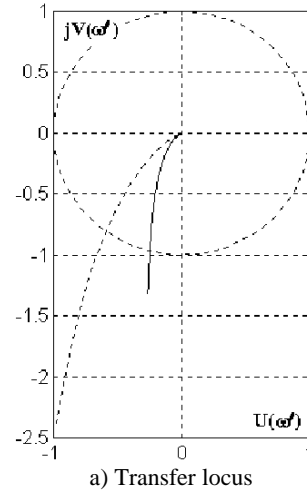
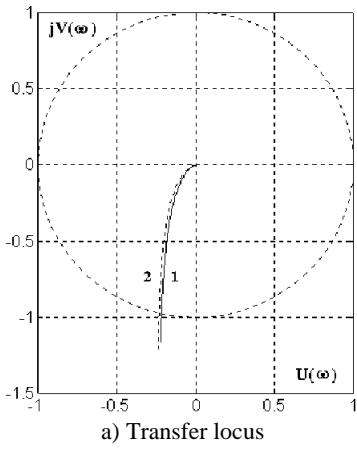


Fig. 2 Graphic dependences corresponding to the cases $R_s=7,5 \Omega$ (continuous line) and $R_s=2,5 \Omega$ (dotted line)

Fig. 3 Graphic dependences corresponding to the cases $R'_r=5,5 \Omega$ (continuous line) and $R'_r=4,5 \Omega$ (dotted line)

Observation 1

In order to obtain the characteristics depicted in the figures 2 and 3 it has been considered that the induction motor has the following parameters:

$$r_s^* = 0,0989; \quad r_r^* = 0,0725; \quad x_s^* = 2,1907; \quad x_r^* = 2,1865;$$

Observation 2

With the help of a specially conceived Matlab program [15] and of the characteristics corresponding to the cases when a parameter from the ones depicted in the second

column of the table I is successively modified (over the initial case), the margins of phase depicted in the third column of the same table are obtained.

TABLE I

ABSOLUTE VALUES AND PHASE MARGINS

Par.	Abs. value [Ω], [H], [kgm ²]	Per unit par.	Per unit value	Phase margin [degree]
R_s	7,5	r_s^*	0,0988	75,54
	2,5		0,0330	74,20
R'_r	5,5	r_r^*	0,0725	75,54
	4,5		0,0593	53,71
L_s	0,529	x_s^*	2,1907	75,54
	0,549		2,2735	69,13
L'_r	0,528	x_r^*	2,1865	75,54
	0,548		2,2694	67,31
L_{sh}	0,498	x_{Im}^*	1,8138	75,76
	0,438		2,0623	75,54
J	0,004	h	32,4	75,54
	0,003		24,3	47,65

The following conclusions can be emphasized, by analyzing the previous results:

- the decrease of the stator winding resistance leads to the stability decrease;
- the rotor resistance decrease has also as an effect, the decrease of the machine stability and conversely;
- the increase of the stator winding inductivity leads to the stability decrease;
- at the same time with the rotor inductivity increase, the system stability decreases;
- the main inductivity increase has a non-stabilizing effect;
- the inertia moment increase contributes to the stability increase.

In order to catch quantitatively these interdependences, the following table can be filled.

TABLE II

PERCENT VARIATIONS OF THE PHASE MARGINS

Parameter	Per cent variation of the parameter	Per cent variation of the phase margin
R_s	66,6	2,04
R'_r	18,2	28,89
L_s	3,64	8,48
L'_r	3,93	10,89
L_{sh}	12,04	0,29
J	25	36,92

IV. EXPERIMENTAL CIRCUIT

In order to confirm the previous conclusions, a series of experimental tests have been performed; a few of them are detailed further on.

Thus, the experimental circuit has the structure depicted in the figure 4 ([5], [7] and [8]).

The notations have the following meaning:

- IM – induction motor;
- VFSC – voltage and frequency static converter;
- DAS – data acquisition board;
- CSB – command and synchronization block;
- PB – protection block;
- MPB – magnetic powder break;

- BCB – brake command block;
- STA 16 – connection block.

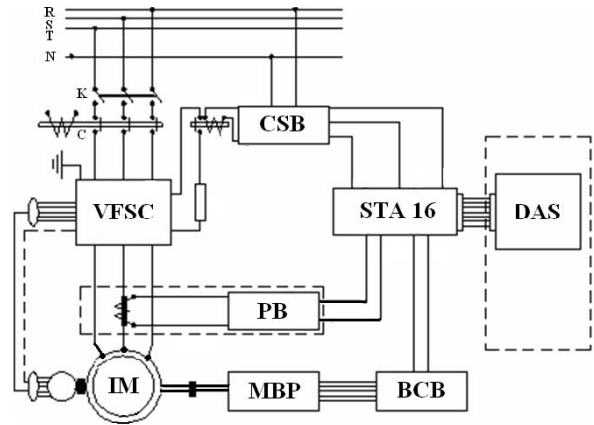


Fig. 4 Scheme of the experimental circuit

A picture of this circuit is depicted for conformity.

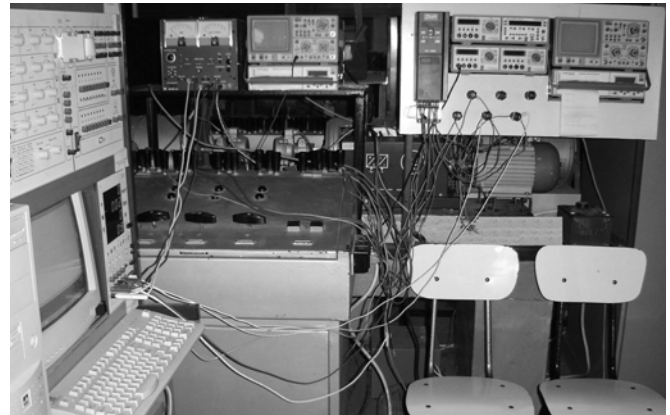


Fig. 5 Picture of experimental circuit

In order to obtain the determinations in dynamic regime the experimental circuit depicted before has been carried out, having a data acquisition board DAS [16] as a central element. This high speed analogical and digital interface has been assembled inside a computer. Both the acquisition and the adequate data processing are controlled with the help of a program conceived in Matlab.

The main characteristics of the board are presented in the following table.

TABLE III
THE CHARACTERISTICS OF THE BOARD DAS

Characteristic	Value
1. Number of analogical inputs	16 unipolar inputs or 8 differential
2. Resolution of the analogical-numerical converter	12 bit
3. Inputs:	
unipolar	0 ÷ +10 V
bipolar	± 10 V
4. Domains selection	By the program
5. Amplifications of the input domains	1, 10, 100, 500
6. Channels D/A (12 bit)	2
7. Digital lines I/O	32 bit

8. Maximum sampling frequency	100 kHz
9. Acquisition time	1,4 ms

The correspondence between the amplification of the input domains, the input type and the maximum rate for scanning several channels so that to obtain the same results as in the case when a single channel is scanned, is emphasized in the following table.

TABLE IV

THE CORRESPONDENCE BETWEEN THE AMPLIFICATION AND THE FREQUENCY			
Amp.	Unipolar	Bipolar	Frequency
1	0 ÷ +10 V	± 10 V	100 kHz
10	0 ÷ +1 V	± 1 V	100 kHz
100	0 ÷ 100 mV	± 100 mV	70 kHz
500	0 ÷ +20 mV	± 20 mV	30 kHz

Data transfer can be made in three ways:

- by direct transfer into the memory without the intermediary micro-processor DMA (Direct Memory Access);
- by subroutine of interruptions;
- by program.

The command and synchronization block CSB ensures the data acquisition starting before the motor starting. The delay occurring between the two moments is then corrected by means of software.

The module PI 200 has been used for adapting the measured currents to the values required by the board. It contains a current transformer in whose secondary there is connected a calibrated resistance; the voltage drop occurring on this resistance is of maximum +10 V.

V. EXPERIMENTAL RESULTS

The graphics depicted in the following figures have been obtained with the help of the previous circuit, for the case of an indirect voltage and frequency static converter voltage source with PWM command and voltage inverter with pre-computed commutation moments.

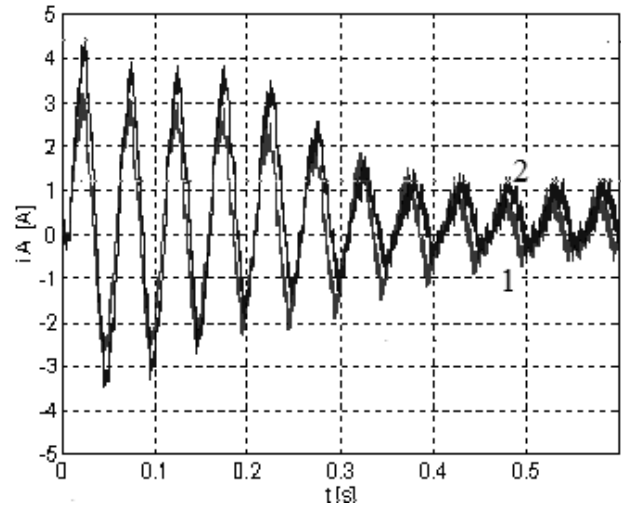


Fig. 6 Graphic dependences corresponding to the cases $R_s=7,5 \Omega$ (1) and $R_s=2,5 \Omega$ (2)

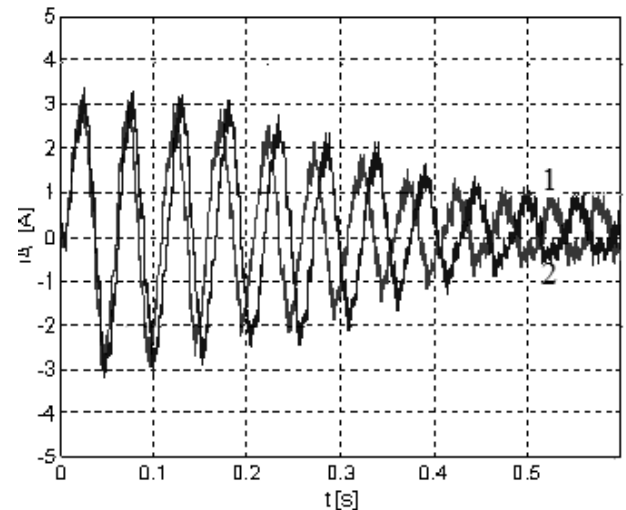


Fig. 7 Graphics dependences corresponding to the cases $R'_s=5,5 \Omega$ (1) and $R'_s=4,5 \Omega$ (2)

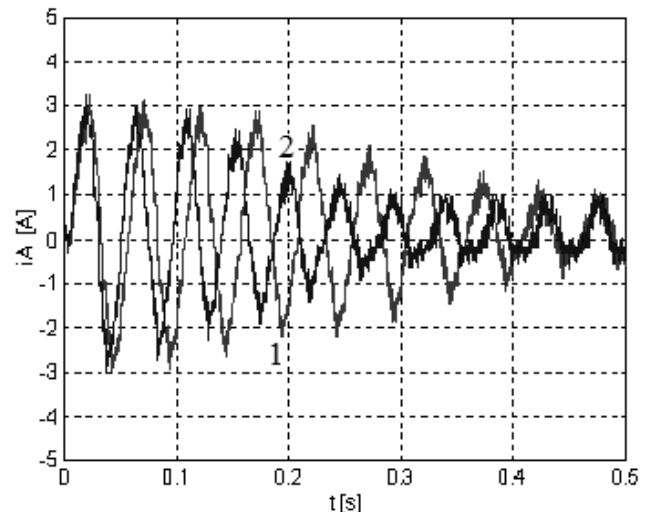


Fig. 8 Graphics dependences corresponding to the cases $J=0,006 \text{ kg.m}^2$ (1) and $J=0,004 \text{ kg.m}^2$ (2)

VI. CONCLUSION

A few interesting conclusions regarding the induction motor parameters influences on the dynamic regime behavior of the analyzed driving systems can be emphasized with the help of the programs detailed before:

- the stator resistance decrease increases very little the duration of the currents transient process and decreases the system stability, respectively;
- the rotor resistance decrease causes the increase of the stabilization time and the stability decrease, respectively;
- when the value of the stator inductance increases the transient process duration increases;
- the rotor inductance value increase also involves the increase of the transient process duration;
- the main inductance decrease determines a faster stabilization of the process (stability increase);
- the inertia moment value increase leads to the increase of the currents stabilization time, and to the stability decrease.

Moreover, when the inverter with pre-established commutation moments is used, it is also noticed that the maximum values of the motor phase currents are modified.

As one can observe, these experimental conclusions confirm the conclusions obtained with the new numerical method for analysis.

REFERENCES

- [1] R. Belmans, L. D'Hondt, "Analysis of the Audible Noise of Three Phase Squirrelcage Induction Motors Supplied by Inverters", *IEEE Transaction on Industry Applications*, Vol. IA-23, 1997, pp. 842-847.
- [2] A. Campeanu, S. Enache, I. Vlad, "Conclusions Regarding Implications of the Induction Motors Parameters on Stability in the Case of Static Converters Supply", in *Proc. of ELECTROMOTION '99*, Patras, Greece, 1999, pp. 373-378.
- [3] B. Delemontey, B. Jacquot, C. Lung, B. De Fornel, J. Bavard, "Stability Analysis and Stabilisation of an Induction Motor Drive with Input Filter", in *Proc. of 6th European Conference on Power Electronics and Applications*, Sevilla, Spain, 1995, pp. 121-126.
- [4] S. Enache, I. Vlad, M.A. Enache, "Considerations Regarding Influences of Induction Motor Resistances upon Stability in case of Operation at Variable Frequency", in *Proc. of SIELMEN'05*, Chisinau, Moldova, 2005, pp. 660-663.
- [5] S. Enache, I. Vlad, *Masina de inductie – Notiuni fundamentale – Procese dinamice*, Ed. Universitaria, Craiova, 2002.
- [6] S. Enache, A. Campeanu, I. Vlad, M. Enache, "A New Method for Induction Motor Stability Analysis when Supplying at Variable Frequency", in *Proc. of WSEAS International Conference on SYSTEMS THEORY AND SCIENTIFIC COMPUTATION*, Athens, 2007, pp. 117-120.
- [7] S. Enache, I. Vlad, M.A. Enache, "Aspects Regarding Dynamic Regimes of Induction Motors Control by the Stator Flux", in *Proc. Of IEEE POWERENG 2007*, Setubal, Portugal, 2007, pp. 152-155.
- [8] S. Enache, R. Prejbeanu, A. Campeanu, I. Vlad, "Aspects Regarding Simulation of the Saturated Induction Motors Control by the Voltage Inverter Commanded in Current", *IEEE Region 8, EUROCON2007 - The International Conference on Computer as a Tool*, Warsaw, Poland, 2007, pp. 1826-1831.
- [9] M.A. Enache M.A., S. Enache, M. Dobriceanu, "Influences of Induction Motor Parameters on Stability in Case of Operation at Variable Frequency", in *Proc. WSEAS International Conference on SYSTEMS THEORY AND SCIENTIFIC COMPUTATION*, Vouliagmeny, Athens, Greece, 2007, pp. 113-116.
- [10] J.L. Lin, L.G. Shiau, "On Stability and Performance of Induction Motor Speed Drives with Slipping Mode Current Control" *Asian Journal of Control*, Vol. 2, No. 2, 2000, pp. 122-131.
- [11] T. Lipo, "Stability Analysis of a Rectifier-inverter Induction Motor Drive", *IEEE Transaction on Industry Applications*, 88, 1, 1993, pp. 57-68.
- [12] H. Mosskull, "Stabilization of an Induction Motor Drive with Resonant Input Filter", in *Proc. 11th European Conference on Power Electronics and Applications*, Dresden, Germany, 2005, pp. 102-107.
- [13] S. Suwankawin, S. Sangwongwanich, "A speed-sensorless IM drive with decoupling control and stability analysis of speed estimation", *IEEE Transactions on Industrial Electronics*, vol. 49, no. 2, 2002, pp. 444-455.
- [14] N. Vinatoru, *Teoria sistemelor*, Ed. Universitaria, Craiova, 1996.
- [15] ***, *Matlab Reference Guide*, The Math Works, Inc., Natick, Massachusetts, 2005.
- [16] ***, *DAS 1601 - Operating Manual*, Keithley Metrabyte, 2002.